Thermophilic α-glucan phosphorylase from *Clostridium thermocellum*: Cloning, characterization and enhanced thermostability

Xinhao Ye [a], Joe Rollin [a], Yi-Heng Percival Zhang [a,b,c,*]

[a] *Biological Systems Engineering Department, Virginia Polytechnic Institute and State University, 210-A Seitz Hall, Blacksburg, VA 24061, USA*
[b] *Institute for Critical Technology and Applied Science (ICTAS), Virginia Polytechnic Institute and State University, 210-A Seitz Hall, Blacksburg, VA 24061, USA*
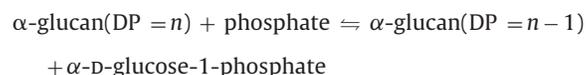[c] *DOE Bioenergy Science Center, Oak Ridge, TN 37831, USA*

ARTICLE INFO

ABSTRACT

ORF Cthe0357 from the thermophilic bacterium *Clostridium thermocellum* ATCC 27405 that encodes a putative α-glucan phosphorylase (αGP) was cloned and expressed in *Escherichia coli*. The protein with a C-terminal His-tag was purified by Ni^{2+} affinity chromatography; the tag-free protein obtained from a cellulose-binding module–intein–αGP fusion protein was purified through affinity adsorption on amorphous cellulose followed by intein self-cleavage. Both purified enzymes had molecular weights of *ca.* 81,000 and similar specific activities. The optimal conditions were pH 6.0–6.5 and 60 °C for the synthesis direction and pH 7.0–7.5 and 80 °C for the degradation direction. This enzyme had broad substrate specificities for different chain length dextrins and soluble starch. The thermal inactivation of this enzyme strongly depended on temperature, protein concentration, and certain addictives that were shown previously to benefit the protein thermostability. The half lifetime of 0.05 mg αGP/mL at 50 °C was extended by 45-fold to 90 h through a combined addition of 0.1 mM Mg^{2+}, 5 mM DTT, 1% NaCl, 0.1% Triton X-100, and 1 mg/mL BSA. The enzyme with prolonged stability would work as a building block for cell-free synthetic enzymatic pathway biotransformations, which can implement complicated biocatalysis through assembly of a number of enzymes and coenzymes.

1. Introduction

α-Glucan phosphorylases (αGP, EC 2.4.1.1) are responsible for catalyzing the reversible phosphorolysis of α-1,4 glucan as shown below:

$$\alpha\text{-glucan(DP} = n) + \text{phosphate} \leftrightharpoons \alpha\text{-glucan(DP} = n - 1)$$
$$+ \alpha\text{-D-glucose-1-phosphate}$$

where DP denotes the degree of polymerization. These enzymes are widely distributed in microorganisms, plants, and animals. They play important roles in carbohydrate metabolism [1,2]. All α-glucan phosphorylases belong to the family 35 glycoyl transferases (www.cazy.org) [3]. Although enzymes from various organisms differ dramatically in their substrate specificity and their modes of regulation, they have similar subunit molecular masses ($\approx$90 kDa), have highly conserved sequences in substrate binding sites and active sites, and require pyridoxal phosphate (PLP) as a cofac-

tor [4,5]. α-glucan phosphorylases can be used for generation of high-yield hydrogen [6–8], synthesis of amylose [9], production of complicated carbohydrates [10,11], and generation of glucose 1-phosphate (G-1-P) for cell-free protein synthesis [12].

Thermophilic enzymes are of importance for industrial applications and molecular biology R&D. In addition to a large number of mesophilic α-glucan phosphorylases that have been characterized from bacteria [13], yeasts [14], fungi, plants, and animal tissues [15,16], several thermostable α-glucan phosphorylases have been purified and characterized from *Aquifex aeolicus* [17], *Geobacillus stearothermophilus* [18], *Sulfolobus tokodaii* [10], *Thermus aquaticus* [19], *Thermus thermophilus* [20], and *Thermotoga maritima* [21]. However, most of them are hyperthermophilic enzymes, which are rarely active at relatively low temperatures [6,22,23]. To our knowledge, only one thermophilic α-glucan phosphorylase gene from *G. stearothermophilus* has been cloned, expressed in *Escherichia coli*, and the protein has been characterized [18]. For reactions in the temperature range of 40–60 °C, it is relatively important to discover more thermophilic α-glucan phosphorylases that can be active and stable as building blocks for cell-free enzymatic biotransformation for a long time (e.g., a week or longer).

Clostridium thermocellum is a thermophilic, anaerobic, Gram-positive bacterium with an optimal growth temperature of *ca.* 60 °C. It is a cellulose specialist, utilizing beta-1,4-glucosidic

bond linked cellodextrins and cellulosic substrates only but neither glucose, maltodextrin nor starch [24]. The *C. thermocellum* cellobiose and cellodextrin phosphorylases (CBP and CDP) play important roles in intracellular cleavage of cellodextrins by generating glucose-1-phosphate without ATP expenditure [25,26]. According to the *C. thermocellum* genome sequence (http://genome.ornl.gov/microbial/cthe/), ORF Cthe0357 (*αgp*) has been annotated to encode a putative α-glucan phosphorylase (αGP). The biochemical and physiological function of the putative αGP in *C. thermocellum* is not clear.

In this work, we cloned the putative *C. thermocellum agp* gene and expressed it in *E. coli*, and characterized the properties of this recombinant enzyme. We also significantly enhanced the half life-time of this enzyme by formulating an enzyme buffer, which would be compatible with its potential applications.

2. Materials and methods

2.1. Chemicals and strains

All chemicals were reagent-grade, purchased from Sigma (St. Louis, MO), unless otherwise noted. *C. thermocellum* ATCC 27405 genomic DNA was a gift from Dr. Jonathan Mielenz at the Oak Ridge National Laboratory (Oak Ridge, TN). *E. coli* DH5α was used for plasmid manipulation; *E. coli* Rosetta BL21 (DE3) containing the gene expression plasmid was employed for producing the recombinant protein. Luria–Bertani (LB) medium was used with 100 μg/mL ampicillin (sodium salt). Microcrystalline cellulose – Avicel PH105 – was purchased from FMC (Philadelphia, PA). Regenerated amorphous cellulose (RAC) with a high external binding capacity was prepared from Avicel after water slurrying, cellulose dissolution in H_3PO_4, and regeneration in water [27]. RAC with a number-average DP of 33 was prepared in concentrated phosphoric acid with partial hydrolysis at 50 °C for 10 h. Dextrin DP4, dextrin DP14, and dextrin DP19 denote maltodextrin with average DPs of 4, 14, and 19, respectively.

2.2. Plasmid construction

ORP Cthe0357 was inserted into two gene expression plasmids pET21c and pCIG, yielding pET21c-*αgp* and pCI-*αgp*, respectively. For the pET21c-*αgp* plasmid, a pair of primers (p1—5′ GGAGG GGAGC TCTGT ATCTT TTTGG AAAAA TTAC 3′ and p2—5′ GAGCG AGCTC AACTG TACAA TCCAT CTGAT AAGTC 3′, SacI site underlined) was employed for PCR amplification based on the genomic DNA. After SacI digestion, the resulting fragment was ligated to the SacI-digested pET21c. After transformation, a clone containing pET21c-*agp* with *agp* in the proper direction was screened by colony PCR and then was validated by DNA sequencing. Plasmid pCI-*αgp* was constructed based on plasmid pCIG [28] by replacing the green fluorescent protein gene (*gfp*) with *αgp* to produce a fusion protein containing a family 3 cellulose-binding module (CBM3), intein, and αGP. The *αgp* gene was amplified with a pair of primers (p3—5′ TGGTG GCTCG AGATG TATCT TTTTG GAAAA ATTAC 3′, XhoI site underlined and p4—5′ AAGAA GGGAT CCTTA CTGTA CAATC CATCT GATAA GTCC 3′, BamHI site underlined) based on the genomic DNA of *C. thermocellum*. The PCR product was digested by XhoI and BamHI, and then ligated with the XhoI/BamHI-digested pCIG vector for plasmid pCI-*αgp*, and the plasmid sequence was validated by DNA sequencing.

2.3. Protein production and purification

E. coli cultures were grown in the LB medium at 37 °C with a rotary shaking rate of 250 rpm. Once the absorbance of the culture reached ~0.8, IPTG was added to a final concentration of 0.25 mM.

After 4 h of cultivation at 37 °C, the *E. coli* cells were harvested by centrifugation and re-suspended in a 50 mM HEPES buffer (pH 7.2). The cells were then lysed by sonication. After centrifugation, the His-tagged αGP in the supernatant was adsorbed to the Bio-Rad Profinity IMAC Ni-resin (Hercules, CA) and was eluted by a 250 mM imidazole buffer. The fusion protein CBM–intein–αGP was specifically bound on RAC. After pH adjustment for intein self-cleavage, the cleaved αGP protein was obtained in the supernatant [28]. Both purified proteins were finally dialyzed against a 50 mM HEPES buffer (pH 7.2) and concentrated by using Centriprep centrifugal filter tubes (Millipore, MA) with a molecular weight cut-off of 50,000.

2.4. Activity assays

The enzyme activities were assayed at 50 °C in 50 mM HEPES buffer (pH 7.20) containing 30 mM dextrin DP19 and 10 mM P_i or G-1-P unless otherwise noted. All enzymatic reactions were conducted in 5-mL glass tubes (12 mm × 75 mm, Fisher Scientific). The reactions were stopped by placing the tubes in a boiling water bath for 5 min. For the synthesis direction, the product—inorganic phosphate released from G-1-P was measured by the mild pH phosphate assay as described elsewhere [29]. For the degradation direction, the product G-1-P was measured by using a glucose hexokinase/glucose-6-phosphate dehydrogenase assay kit [25] supplemented with a recombinant phosphoglucomutase [23].

2.5. Optimization of αGP reaction conditions

The effects of metal ions and reagents on αGP activity were examined, and the concentration of potential activators were optimized for both synthesis and degradation directions. The pH effects on the enzyme activities in both directions were determined in 50 mM acetate buffers (pH 3.0–6.0), HEPES buffers (pH 6.5–8.0), and Na_2CO_3–$NaHCO_3$ buffers (pH 9.0–10.0). The temperature ranges of the enzymes were tested from 10 to 90 °C.

2.6. Enzyme kinetics

For the synthesis direction, kinetic parameters were determined based on the initial rates by measuring the release of inorganic phosphate. The reactions were conducted at 50 °C in a 50 mM HEPES buffer (pH 6.8) containing 1 mM Mg^{2+}, 5 mM DTT, and various substrate concentrations between 0.2 and 5 times of their respective K_m values. Typical enzyme concentrations were 9 and 90 μg/mL on starch or dextrin and on RAC, respectively. One unit of phosphorylase in the synthesis direction was defined as the amount of enzyme that generated one micromole of phosphate per min. For the degradation direction, the reactions were conducted at 50 °C in a 50 mM HEPES buffer (pH 7.2) containing 3 mM Mg^{2+}, 1 mM DTT, and G-1-P at different concentrations. The enzyme concentration was 17.8 μg/mL. One unit of phosphorylase in the degradation direction is defined as the amount of enzyme generating one micromole of G-1-P per min.

2.7. Thermostability

The thermostability of αGP was studied at 40, 50, 60, 70, and 80 °C. The purified enzyme (0.01, 0.05, 0.25 mg/mL) was incubated in a 50 mM HEPES buffer (pH 7.2) without and with 0.1 mM Mg^{2+}, 5 mM DTT, 1% NaCl, 0.1% Triton X-100, and 1 mg/mL BSA at different temperatures for different time periods. The residual enzyme activities were assayed in the direction of dextrin degradation at 50 °C in a 50 mM HEPES buffer (pH 7.2) containing 5 μg/mL αGP, 30 mM dextrin DP19, 10 mM P_i, 3 mM Mg^{2+}, and 1 mM DTT.

Table 1
Purification of the αGP from *C. thermocellum*.

Fraction	Volume (mL)	Total protein (mg)	Total activity[a] (U)	Sp. act. (U/mg)	Yield (%)
His$_6$-tagged enzyme					
Crude extract	23	40.1	27.2	0.678	100
Fraction eluted from Ni^{2+} resin	15	6.18	13.5	2.18	49.6
Dialysis and concentration	6.1	5.36	11.9	2.22	43.8
Tag-free enzyme					
Crude extract	26	44.1	22.7	0.515	100
Fraction truncated by intein self-cleavage	6.5	3.74	7.47	2.00	32.9
Dialysis and concentration	3.2	3.16	6.57	2.08	

[a] The activity was assayed in the synthesis direction at 50 °C in a 50 mM HEPES buffer (pH 6.8) containing 30 mM dextrin DP19 and 10 mM G-1-P.

2.8. Other assays

Protein mass concentrations were determined by the Bradford methods with bovine serum albumin (BSA) as the standard. The number average degree of polymerization of RAC was determined as described elsewhere [30]. The purity of the enzymes was checked by SDS PAGE.

3. Results and discussion

3.1. Sequence analysis

A 2569-bp *C. thermocellum* ORF Cthe0357 was annotated to encode a putative α-glucan phosphorylase, according to BLASTP analysis [31]. The deduced amino acid sequence has 43% identity with the hyperthermophilic *Thermotoga maritima* αGP, 23% identity with the thermophilic *G. stearothermophilus* αGP, and 22% identity with the mesophilic *E. coli* maltodextrin phosphorylase (MalP). The domain from residues 114 to 705 has 95% identity to the conserved domains (CDS) of family 35 glycoyl transferases—α-glucan phosphorylases. Compared to the β-glucan phosphorylases from family 94 glycoside hydrolases, such as *C. thermocellum* cellobiose phosphorylase and cellodextrin phosphorylase, the identities were only 6.0% and 6.4%, respectively. This analysis suggested that Cthe0357 encoded an α-glucan phosphorylase.

3.2. Protein production and purification

Two expression plasmids, pET21c-αgp and pCI-αgp, were constructed for the production of His-tagged and tag-free α-glucan phosphorylase, respectively. The purified His-tagged αGP appeared to be homogeneous with a molecular mass of *ca.* 81 kDa (Fig. 1), which was close to the estimated value of 97,712 Da from the deduced amino acid sequence. The purified enzyme had a specific activity of 2.22 ± 0.17 U/mg and the purification yield was 43.8% (Table 1). Approximately 10.8 mg of the purified enzyme was obtained per liter of the culture.

The tag-free phosphorylase was purified by affinity adsorption of the fusion protein containing a CBM3 tag on an ultra-high capacity adsorbent RAC, followed by intein self-cleavage. The specific activity of the tag-free phosphorylase was 2.08 ± 0.23 U/mg with a yield of 28.9% (Table 1). Approximately 6.4 mg of the purified phosphorylase was obtained per litre of the culture. The relatively low purification yield of the CBM3–intein-based protein purification was mainly attributed to self-cleavage of the intein *in vivo*. Higher yield could be achieved through short-time protein production at low temperature [28]. SDS PAGE analysis indicated that the purified tag-free phosphorylase was homogenous and had a molecular mass of ~81 kDa similar to the His-tagged protein (Fig. 1, lanes 2 and 5). Since the two forms of phosphorylase had similar specific activities, the His-tagged phosphorylase was used for further characterization.

3.3. Biochemical properties

The effects of metal ions, including Mn^{2+}, Mg^{2+}, Ca^{2+}, Cu^{2+}, Zn^{2+}, and Ni^{2+}, and reagents, including EDTA, AMP, and DTT, on αGP activity were examined. The highest activity was obtained in the presence of 1 mM Mg^{2+} and 5 mM DTT for the synthesis direction, resulting in 1.4-fold increase in αGP activity as compared to those without addition of metal ions or DTT. But the highest activity in the degradation direction was obtained in the presence of 3 mM Mg^{2+} plus 1 mM DTT, 1.7-fold higher than the blank control. One millimolar Mn^{2+} strongly inhibited αGP activity, decreasing the activity more than 90%. The other metals (1 mM) or AMP (1 mM) or EDTA (1 mM) had no significant influences on its activities. However, high level Ca^{2+} and Ni^{2+} caused obvious salt precipitates and 10 mM EDTA decreased its activities by *ca.* 30%.

Fig. 2A shows the effects of pH from 3.0 to 10.0. The maximal activity was found at pH 6.0–6.5 and 7.0–7.5 in the synthesis and degradation directions, respectively (Fig. 2A). Different pH preferences for different reaction directions were also reported for the αGP from *Corynebacterium callunae*, which had pH optima at 5.7–6.1 and 7.0–7.2 in the synthesis and degradation directions, respectively [5].

The effect of temperature was investigated from 10 to 90 °C at pH 7.2. For the synthesis direction, the optimal temperature was 60 °C; this enzyme retained nearly 97% of its activity at 50 °C (Fig. 2B). For the degradation direction, the optimal temperature was 80 °C. The enzyme activity sharply declined when the temperatures were higher or lower than 80 °C (Fig. 2B). The activation energies were 25.3 and 42.9 kJ/mol for the degradation and synthesis directions, respectively, according to the Arrhenius plots.
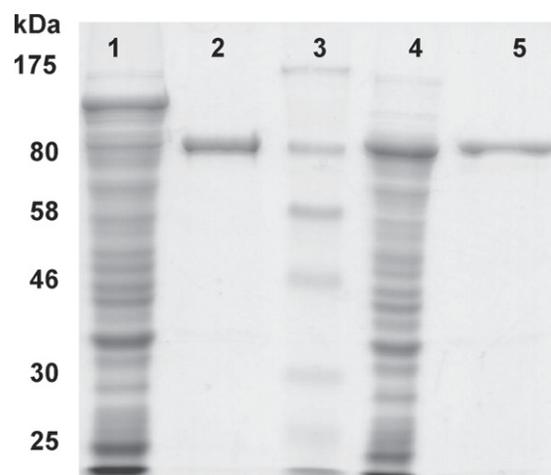

Fig. 1. Purification of His-tagged and non-tagged *C. thermocellum* αGP. Lane 1, crude cell extracts from *E. coli* containing the CBM3–intein–αGP fusion protein; lane 2, final purified tag-free protein; lane 3, molecular weight marker; lane 4, crude cell extracts from *E. coli* containing His-tagged αGP; lane 5, purified His-tagged protein.

Table 2
Apparent kinetics constants of *C. thermocellum* αGP in the directions of glucan synthesis and degradation.

Variable substrate	Fixed substrate	k_{cat} (s^{-1})	K_m (mM)[a]	k_{cat}/K_m (M^{-1} s^{-1})
Synthesis[b]				
Dextrin DP19	10 mM g1p	6.6 ± 0.3	1.9 ± 0.2	0.0035
Dextrin DP14	10 mM g1p	3.6 ± 0.1	1.2 ± 0.2	0.0030
Dextrin DP4	10 mM g1p	11.0 ± 0.4	17.1 ± 0.2	0.00064
Starch[c]	10 mM g1p	2.1 ± 0.2	1.5 ± 0.2	0.0015
Glucose 1-phosphate	40 mM dextrin 19	4.2 ± 0.1	0.054 ± 0.008	0.0077
RAC DP33	10 mM g1p	0.12 ± 0.05	0.72 ± 0.18	0.00017
Degradation[d]				
Dextrin DP19	30 mM P$_i$	8.1 ± 0.2	0.39 ± 0.01	0.021
Dextrin DP14	30 mM P$_i$	9.3 ± 0.3	0.73 ± 0.03	0.013
Dextrin DP4	30 mM P$_i$	8.4 ± 0.8	1.8 ± 0.2	0.0047
Starch[c]	30 mM P$_i$	6.3 ± 0.6	0.30 ± 0.07	0.021
P$_i$	40 mM dextrin 19	8.2 ± 0.5	7.7 ± 0.6	0.0011
RAC DP33	30 mM P$_i$	ND[e]	ND[e]	ND[e]

[a] The concentration of polysaccharides were given as the molar concentration of the non-reducing ends.
[b] The activities were assayed at 50 °C in a 50 mM HEPES buffer (pH 6.8) containing 1 mM Mg^{2+}, 5 mM DTT and various substrate concentrations between 0.2 and 5 times of their respective K_m values.
[c] The DP of soluble starch was estimated to be 24.
[d] The activities were conducted at 50 °C in a 50 mM HEPES buffer (pH 7.2) containing 3 mM Mg^{2+} and 1 mM DTT at various substrate concentrations.
[e] Not detected.
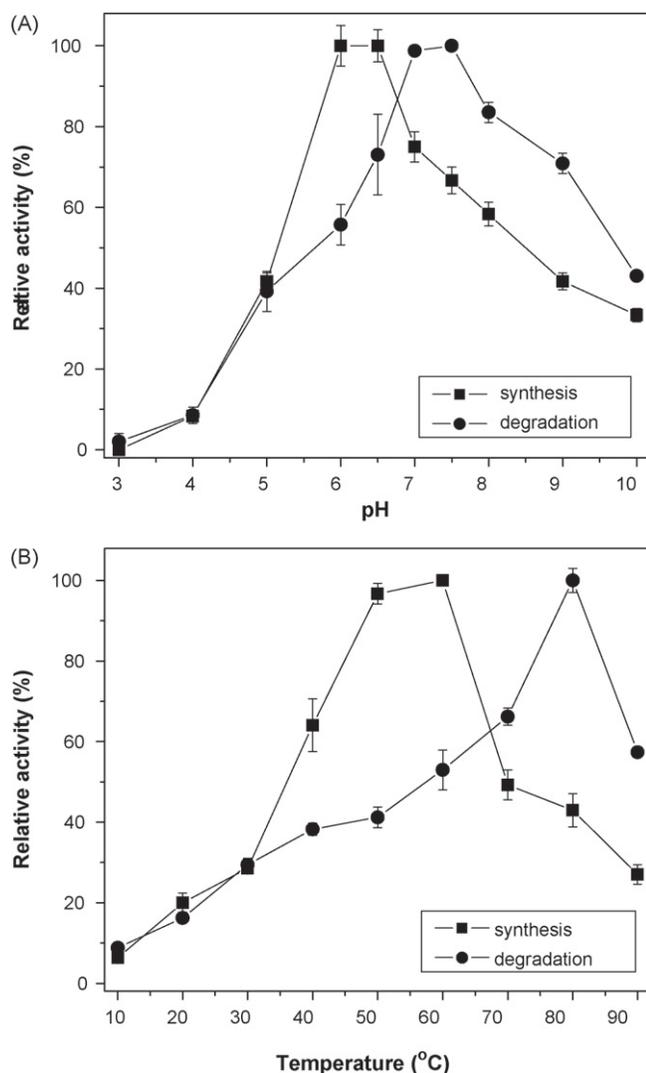
Fig. 2. The profiles of pH (A) and temperature (B) of the *C. thermocellum* αGP.

Different optimal pH and temperatures suggested partially different binding and reaction modes in synthesis and degradation [32], but different pH and temperature optima have often been ignored in studies of αGP [10,17,18].

3.4. Substrate specificity and kinetics

The substrate specificity and kinetics of αGP were determined in the synthesis and degradation directions on different substrates (dextrin DP19, dextrin DP14, dextrin DP4, soluble starch, and RAC DP33) (Table 2). In the synthetic direction, there were no significant differences between the kinetic parameters on dextrin DP14 and dextrin DP19. When the substrate chain length decreased to 4, the K_m value increased 14-fold, to 17.1 mM. Consequently, enzyme efficiency (k_{cat}/K_m = 0.00064 M^{-1} s^{-1}) on dextrin DP4 was approximately 5-fold lower than that on dextrin DP14 (0.0030 M^{-1} s^{-1}) although k_{cat} on dextrin DP4 (11.0 s^{-1}) was higher than on dextrin DP14 (3.6 s^{-1}). The similar trend for K_m was found in the degradation direction. αGP exhibited similar kinetic properties for dextrin DP14 and DP19, and had a lower catalytic efficiency on the shorter substrate dextrin DP4. These results indicated that the *C. thermocellum* α-glucan phosphorylase preferred substrates with DP > 4 for both synthetic and phosphorolytic reactions.

The *C. thermocellum* α-glucan phosphorylase showed broad substrate specificities from soluble dextrin to starch. The catalytic efficiencies on dextrins (with DP > 4) and starch were comparable. αGP did not work on amorphous cellulose (RAC DP33, cellulosic materials linked by beta-1,4-glucosidic bonds) in the degradation direction but it had a weak activity in the synthesis direction (k_{cat}/K_m = 0.00017 M^{-1} s^{-1}). Such special properties implied that the enzyme might be responsible for the formation of glycocalyx in *C. thermocellum* [24].

3.5. Thermostability

Fig. 3A shows that αGP deactivation was strongly associated with its concentration. After being incubated at 50 °C for 2 h, more than 60% and 85% of αGP activities remained for enzyme concentrations of 0.05 and 0.25 mg/mL, respectively, but αGP at a low concentration (0.01 mg/mL) had less than 5% of its initial activity. The half lifetimes of 0.05 mg/mL αGP were around 125, 84, 37, and 4 min at 50, 60, 70, and 80 °C, respectively (Fig. 3B). At 40 °C, the enzyme was relatively stable with more than 90% activity remaining after a 2 h heat treatment.
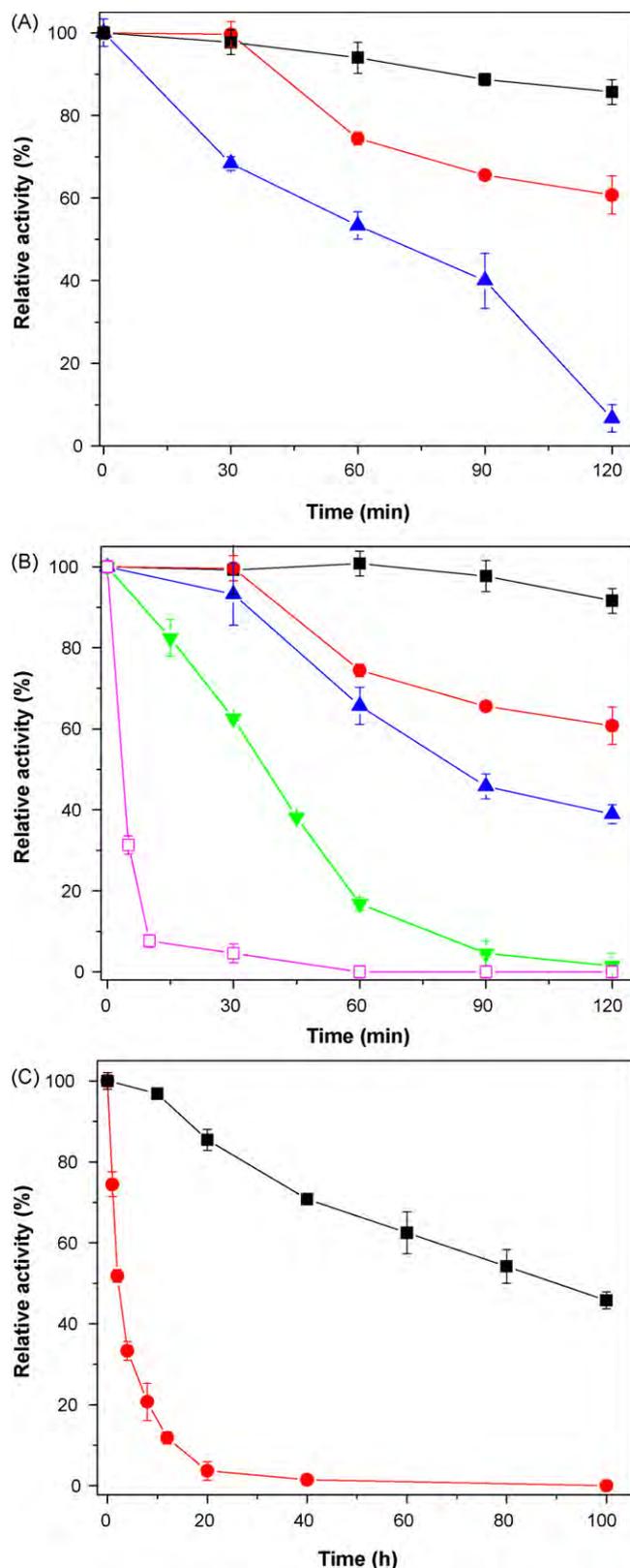
Fig. 3. Thermostability of the *C. thermocellum* αGP. (A) Thermostability of αGP at different protein concentrations of 0.01, 0.05, 0.25 mg/mL at 50 °C. 0.01 mg/mL (▲), 0.05 mg/mL (●), and 0.25 mg/mL (■); (B) thermostability of 0.05 mg/mL αGP at 40 °C (■), 50 °C (●), 60 °C (▲), 70 °C (▼), and 80 °C (□); (C) thermostability of 0.05 mg/mL αGP without additives (●), and with addition of 0.1 mM Mg^{2+}, 5 mM DTT, 1% NaCl, 0.1% Triton X-100, and 1 mg/mL BSA (■) at 50 °C. The residual enzyme activities were assayed in the degradation direction as described in Section 2. (For interpretation of the references to color in this figure legend, the reader is referred to the web version of the article.)

Stabilization of αGP at low concentrations would be important for its potential applications. A myriad of efforts have been made to improve αGP thermostability through immobilization [33], protein engineering *via* directed evolution [34] or rational design [35], protein formulation [36], and with the help of folding chaperones [37]. Compared to these methods, the enhancement of protein thermal inactivation through the addition of protective reagents is easier, but this strategy is often ignored [23]. Therefore, a number of combinations of various concentrations of Mg^{2+}, DTT, NaCl, Triton X-100, and BSA were tested. The presence of metal ions and the reducing agent DTT was reported to reduce the disulfide bridges and suppress thiol/disulfide (SH/SS) interchange—a major cause of enzyme deactivation [38]. Magnesium ions may protect the enzyme from thermal denaturation [39]. High concentration salts are capable of preventing protein aggregation as well as thermally induced unfolding [40]. Triton X-100 has been widely used to stabilize DNA polymerases for PCR, nucleic acid hybridization, and enzyme storage, although its real function remains unclear [23]. After testing, a combination of 0.1 mM Mg^{2+}, 5 mM DTT, 1% NaCl, 0.1% Triton X-100, and 1 mg/mL BSA was found to keep the activity of αGP unchanged but to extend the half time of inactivation by 45-fold from ∼2 h to *ca.* 90 h at 50 °C (Fig. 3C).

3.6. Homology modeling and structural analysis

A homology model of the *C. thermocellum* α-glucan phosphorylase was built by using 3D-JIGSAW based on the human liver glycogen phosphorylase (HLGP, PDB: 1l7×), as shown in Fig. 4. The crystal structure of HLGP was used as a template because it has the highest identity (23%) with the *C. thermocellum* αGP based on their catalytic domains. The *C. thermocellum* αGP shares some similar structural properties with HLGP around the catalytic sites. For example, the catalytic domain of HLGP is formed by the 250's loop (residues 250–260), the GATE (residues 280–289), and the 380's loop (residues 376–386) (Fig. 4A) [41,42]. Similarly, the catalytic domain of the *C. thermocellum* αGP is composed of the 215's loop (residues 215–225), the GATE (residues 239–248), and the 315's loop (residues 315–325) (Fig. 4B). The key residues, involving in intermolecular contacts for enzyme–substrate complex, appear identical in HLGP and αGP, such as His377 (HLGP) to His315 (αGP) for sugar subsite −1, Asn339 (HLGP) to Asp276 (αGP) for sugar subsite +1, Tyr280 and His341 (HLGP) to Tyr241 and His279 (αGP) for sugar subsite +2, Arg 292 (HLGP) to Arg 248 (αGP) for sugar subsite +3, and Pro381 (HLGP) to Pro319 (αGP) for sugar subsite +4 [41,43]. The homology model clearly suggests that the *C. thermocellum* αGP has a five glucose unit binding site (subsites −1 to +4), similar to HLGP. It is also supported by our experimental data that Michaelis–Menten constant (K_m) significantly decreased as substrate chain lengths were longer than four (Table 2).

Some differences between the HLGP structure and the *C. thermocellum* αGP model were observed, e.g. in the region of helix 2 (residues 48–78 of HLGP) and 'CAP' (residues 42–45 of HLGP, so-called because it 'caps' the AMP binding site) [42]. Helix 2 and CAP structures are believed to form the binding site of AMP which is an efficient activator for HLGP [44]. Hence, the big structural differences in the helix 2 and CAP between HLGP and αGP may explain why AMP, a regulator for most eukaryotic α-glucan phosphorylases, has no influence on the activity of the *C. thermocellum* αGP. Such changes also result in dramatic differences in the catalytic machinery between them. HLGP has two conformational states: a less active T state and a more active R state. In the T state, 280's loop and GATE block access to the catalytic site and create an unfavorable electrostatic environment at the catalytic site for phosphate ions [41]. Once it binds with AMP or is phosphorylated at Ser14, HLGP is switched to the active R state [45,42]. By contrast, the 215's loop and GATE structures of *C. thermocellum* αGP seem to be an open
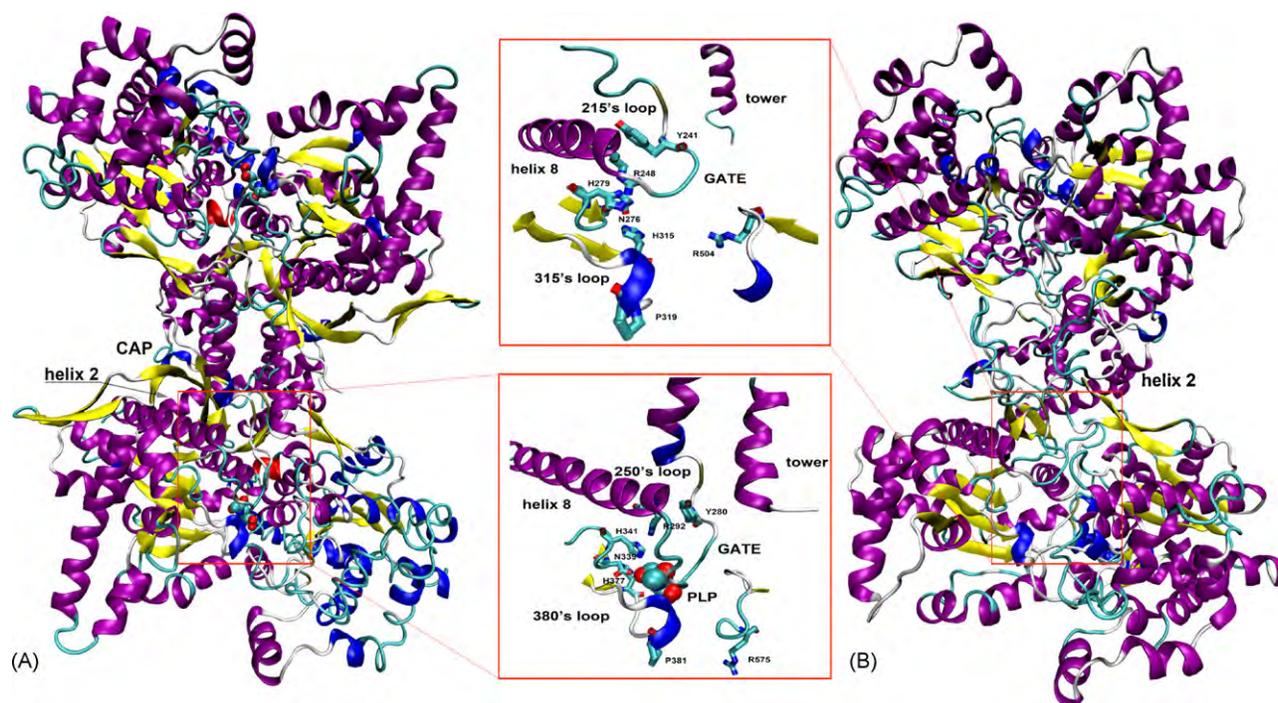
Fig. 4. Comparison of the crystal structure of human liver glycogen phosphorylase (HLPG) (A) and a homology model of *C. thermocellum* αGP (B). The protein structures were illustrated by VMD (UIUC, IL, USA), where α-helices, 3_{10}-helices, extended β-stands, bridge β-stands, turns, and coils were colored by purple, blue, yellow, tan, cyan and white, respectively. CAP: a subunit (residues 42–45) of HLGP which caps the AMP binding site; GATE: a subunit (residues 280–289 in HLGP, and residues 239–248 in αGP) that takes a critical role in substrate binding; PLP, pyridoxal phosphate. (For interpretation of the references to color in this figure legend, the reader is referred to the web version of the article.)

conformation always (Fig. 4). It allows the substrate to access the catalytic site so that the *C. thermocellum* αGP is constantly active.

4. Conclusion

ORF Cthe0357 from *C. thermocellum*, which encodes an α-glucan phosphorylase, was cloned and expressed in *E. coli*. The recombinant enzyme showed broad substrate specificities on dextrin and starch. Although its physiological role is still unclear, it may be responsible for the formulation of glycocalyces. Through buffer formulation, the half lifetime of this enzyme was extended by 45-fold to *ca.* 90 h at 50 °C. Therefore, the enzyme has the potential for broad applications in cell-free protein synthesis [46] and biofuels production *via* cell-free synthetic enzymatic pathway biotransformation [47,48].

References

[1] R.J. Fletterick, N.B. Madsen, Annu. Rev. Biochem. 49 (1980) 31–61.
[2] C.B. Newgard, P.K. Hwang, R.J. Fletterick, Crit. Rev. Biochem. Mol. Biol. 24 (1989) 69–99.
[3] B.L. Cantarel, P.M. Coutinho, C. Rancurel, T. Bernard, V. Lombard, B. Henrissat, Nucl. Acids Res. 37 (2009) D233–238.
[4] R. Schinzel, B. Nidetzky, FEMS Microbiol. Lett. 171 (1999) 73–79.
[5] A. Weinhausel, R. Griessler, A. Krebs, P. Zipper, D. Haltrich, K.D. Kulbe, B. Nidetzky, Biochem. J. 326 (1997) 773–783.
[6] X. Ye, Y. Wang, R.C. Hopkins, M.W.W. Adams, B.R. Evans, J.R. Mielenz, Y.H.P. Zhang, ChemSusChem 2 (2009) 149–152.
[7] Y-H.P. Zhang, Biotechnol. Bioeng. (2010), doi:10.1002/bit.22630.
[8] Y.H.P. Zhang, B.R. Evans, J.R. Mielenz, R.C. Hopkins, M.W.W. Adams, PLoS ONE 2 (2007) e456.
[9] K. Ohdan, K. Fujii, M. Yanase, T. Takaha, T. Kuriki, J. Biotechnol. 127 (2007) 496–502.
[10] Y. Hong, L. Wu, B. Liu, C. Peng, D. Sheng, J. Ni, J. Shen, J. Mol. Catal. B: Enzym. 54 (2008) 27–34.
[11] M. Yanase, T. Takaha, T. Kuriki, J. Sci. Food Agric. 86 (2006) 1631–1635.
[12] Y. Wang, Y.H.P. Zhang, BMC Biotechnol. 9 (2009) 59.
[13] G. Chen, I. Segel, Arch. Biochem. Biophys. 127 (1968) 175–186.
[14] V.L. Rath, P.K. Hwang, R.J. Fletterick, J. Mol. Biol. 225 (1992) 1027–1034.
[15] T. Fukui, S. Shimomura, K. Nakano, Mol. Cell. Biochem. 42 (1982) 129–144.
[16] P.V. Rogers, S. Luo, J.F. Sucic, C.L. Rutherford, BBA–Gene Struct. Expr. 1129 (1992) 262–272.
[17] S.H. Bhuiyan, A.A. Rus'd, M. Kitaoka, K. Hayashi, J. Mol. Catal. B: Enzym. 22 (2003) 173–180.
[18] H. Takata, T. Takaha, S. Okada, M. Takagi, T. Imanaka, J. Ferment. Bioeng. 85 (1998) 156–161.
[19] T. Takaha, M. Yanase, H. Takata, S. Okada, J. Appl. Glycosci. 48 (2001) 71–78.
[20] B. Boeck, R. Schinzel, Eur. J. Biochem. 239 (1996) 150–155.
[21] M. Bibel, C. Brettl, U. Gosslar, G. Kriegshäuser, W. Liebl, FEMS Microbiol. Lett. 158 (1998) 9–15.
[22] T. Suzuki, M. Yasugi, F. Arisaka, A. Yamagishi, T. Oshima, Protein Eng. 14 (2001) 85–91.
[23] Y. Wang, Y-H.P. Zhang, J. Appl. Microbiol. 108 (2010) 39–46.
[24] L.R. Lynd, P.J. Weimer, W.H. van Zyl, I.S. Pretorius, Microbiol. Mol. Biol. Rev. 66 (2002) 506–577.
[25] Y.H.P. Zhang, L.R. Lynd, Appl. Environ. Microbiol. 70 (2004) 1563–1569.
[26] Y.H.P. Zhang, L.R. Lynd, Proc. Natl. Acad. Sci. U.S.A. 102 (2005) 7321–7325.
[27] Y.H.P. Zhang, J.B. Cui, L.R. Lynd, L.R. Kuang, Biomacromolecules 7 (2006) 644–648.
[28] J. Hong, Y. Wang, X. Ye, Y.-H.P. Zhang, J. Chromatogr. A 1194 (2008) 150–154.
[29] S. Saheki, A. Takeda, T. Shimazu, Anal. Biochem. 148 (1985) 277–281.
[30] Y.H.P. Zhang, L.R. Lynd, Biomacromolecules 6 (2005) 1510–1515.
[31] S.F. Altschul, T.L. Madden, A.A. Schaffer, J. Zhang, Z. Zhang, W. Miller, D.J. Lipman, Nucl. Acids Res. 25 (1997) 3389–3402.
[32] P. Drueckes, B. Boeck, D. Palm, R. Schinzel, Biochemistry 35 (1996) 6727–6734.
[33] W. Friedrich, L. Dietmar, W. Kurt, Biotechnol. Bioeng. 19 (1977) 1387–1403.
[34] M. Yanase, H. Takata, K. Fujii, T. Takaha, T. Kuriki, Appl. Environ. Microbiol. 71 (2005) 5433–5439.
[35] R. Griessler, S. D'Auria, R. Schinzel, F. Tanfani, B. Nidetzky, Biochem. J. 346 (2000) 255–263.
[36] S. Janecek, Proc. Biochem. 28 (1993) 435–445.
[37] T.B. Eronina, N.A. Chebotareva, S.G. Bazhina, V.F. Makeeva, S.Y. Kleymenov, B.I. Kurganov, Biophys. Chem. 141 (2009) 66–74.
[38] M. Meng, M. Bagdasarian, J.G. Zeikus, Biotechnology 11 (1993) 1157–1161.

[39] W. Liu, A. Zhang, Y. Cheng, H. Zhou, Y. Yan, FEBS Lett. 581 (2007) 1047–1052.
[40] W.R. Cannon, G. MacDonald, Biophys. J. 96 (2009) 81–82.
[41] M. O'Reilly, K. Watson, R. Schinzel, D. Palm, L. Johnson, Nat. Struct. Biol. 4 (1997) 405–412.
[42] V.L. Rath, M. Ammirati, P.K. LeMotte, K.F. Fennell, M.N. Mansour, D.E. Danley, T.R. Hynes, G.K. Schulte, D.J. Wasilko, J. Pandit, Mol. Cell 6 (2000) 139–148.
[43] K.A. Watson, C. McCleverty, S. Geremia, S. Cottaz, H. Driguez, L.N. Johnson, EMBO J. 18 (1999) 4619–4632.
[44] V. Maddaiah, N. Madsen, J. Biol. Chem. 241 (1966) 3873–3881.
[45] V.L. Rath, M. Ammirati, D.E. Danley, J.L. Ekstrom, E.M. Gibbs, T.R. Hynes, A.M. Mathiowetz, R.K. McPherson, T.V. Olson, J.L. Treadway, et al., Chem. Biol. 7 (9) (2000) 677–682.
[46] Y. Wang, Y.H.P. Zhang, Microb. Cell Fact. 8 (2009) 30.
[47] Y-H.P. Zhang, Energy Environ. Sci. 2 (2) (2009) 272–282.
[48] Y.H.P. Zhang, X. Ye, Y. Wang, in: F. Richter (Ed.), Biotechnology: Research, Technology and Applications, Nova Science Publishers, Hauppauge, NY, USA, 2008.